SERI/STR-211-2804
(DE85016893)

STABLE, HIGH-EFFICIENCY, $CuInSe_2$ –BASED POLYCRYSTALLINE THIN-FILM TANDEM SOLAR CELLS

Annual Subcontract Report for the Period March 16, 1984–March 15, 1985

By
R. W. Birkmire
J. E. Phillips

November 1985

Work Performed Under Contract No. AC02-83CH10093

University of Delaware
Newark, Delaware

and

Solar Energy Research Institute
Golden, Colorado

Technical Information Center
Office of Scientific and Technical Information
United States Department of Energy

DISCLAIMER

Available from the National Technical Information Service, U. S. Department of Commerce, Springfield, Virginia 22161.

Price: Printed Copy A04
Microfiche A01

Codes are used for pricing all publications. The code is determined by the number of pages in the publication. Information pertaining to the pricing codes can be found in the current issues of the following publications, which are generally available in most libraries: *Energy Research Abstracts (ERA); Government Reports Announcements* and Index *(GRA* and I); *Scientific and Technical Abstract Reports (STAR);* and publication NTIS-PR-360 available from NTIS at the above address.

Printed in the United States of America
USDOE Office of Scientific and Technical Information
Oak Ridge, Tennessee

SERI/STR-211-2804
(DE85016893)
Distribution Category UC-63

Stable, High-Efficiency, $CuInSe_2$ - Based Polycrystalline Thin-Film Tandem Solar Cells

Annual Subcontract Report
16 March 1984 - 15 March 1985

R. W. Birkmire
J. E. Phillips
Principal Investigators

Institute of Energy Conversion
University of Delaware
Newark, Delaware

November 1985

Prepared under Subcontract No. XL-4-04025-1
SERI Technical Monitor: R. Mitchell

Solar Energy Research Institute
A Division of Midwest Research Institute

1617 Cole Boulevard
Golden, Colorado 80401

Prepared for the
U.S. Department of Energy
Contract No. DE-AC02-83CH10093

TABLE OF CONTENTS

TABLE OF CONTENTS (cont'd).

* Appendices A through J are available on request from the Institute of Energy Conversion. Please specify the Annual Report on XL-4-04025-1.

ABSTRACT

The goal of this program is a high-efficiency, thin-film tandem solar cell based on $CuInSe_2$. The performance of the (CdZn)S/$CuInSe_2$ component in the tandem has been brought up to an efficiency of well over 10%.[2] Significant improvement in a CdS/CdTe thin-film cell compatible with the tandem design has also been achieved. A number of tandem devices have been made and progress continues on increasing the efficiency of the cells presently being produced.

1. Introduction

At the end of the previous contract, #XL-3-03065-01, an operating monolithic tandem cell based on $CuInSe_2$ had been demonstrated. The low band gap cell was a $CdS/CuInSe_2$ heterojunction onto which the high band gap cell, a CdS/CdTe heterojunction, was deposited by physical vapor deposition. Cell preparation processes had been established at IEC for the component junctions which were yielding a conversion efficiency of about 8% for the $CuInSe_2$ cell and about 5% for the CdTe cell. An initial effort to produce tandem devices had yielded working cells with efficiencies of about 3%. However open circuit voltages of over 1 V had been obtained and the major performance limiting features of the devices being produced had been identified. These were all associated with the CdS/CdTe cell itself and the interconnect to the bottom cell.

During this year substantial progress has been made with all components of the tandem device. Optimization of the $CuInSe_2$ cell has raised the maximum efficiency to well over 10% and the degree of reproducibilty from run-to-run has also reached a very high level. The research on this cell is now focussed on optimizing it for use in the tandem while maintaining, or possibly slightly improving, its individual performance. Among the aspects under investigation is the texture of the top surface which acts as the substrate for the CdTe layer.

The major research effort for most of the year has been addressed at the CdS/CdTe component of the tandem which is

limiting the overall efficiency. Various dopants have been explored and some success achieved using small additions of Hg during film growth. Severely limiting the rate of progress has been the excessive degree of scatter in device performance for nominally identical experimental conditions, in marked contrast to the $CuInSe_2$ cell. Nevertheless progress has been made and efficiencies over 6% achieved. As essentially empirical knowledge of this cell structure is acquired it is expected that progress will continue and efficiencies will reach those reported using other deposition processes.

Although the focus of the experimental work has been the individual CdS/CdTe cell a number of tandem structures have been produced and tested. Optical measurements have revealed unacceptably high losses through the upper layers of the cell and this problem will be addressed during the second year of the program. The experience with actual tandem cells has, as would be expected, revealed features of the $CuInSe_2$ cell which are of no consequence to the isolated junction but which adversly affect the combined cell. During the coming year the coordinated attack on the individual junctions and the tandem structure will continue and is expected to result in a marked improvement in the tandem performance.

2. (CdZn)S/$CuInSe_2$ Cell Development

At the end of the previous contract(1) (CdZn)S/$CuInSe_2$ cells of about 7.5% efficiency were being produced. Systematic progress has been made during this reporting period resulting in arrays of small area cells averaging over 9% efficiency. Immediately following the end of this contract year, arrays averaging 10% were being produced. 1 cm^2 area cells of about 9% efficiency were also produced during the year(4). Contributing to improved efficiencies was the use of thinner CdS layers which allow higher short circuit currents and a progressive optimization of the various cell processing steps.

2.1 Film Growth

The basic techniques for the deposition of $CuInSe_2$ layers continues to be as described in Appendix J of Reference 1. No major modifications to the internal configuration of the evaporator have been made. About four depositions per week are made and the composition monitored routinely using EDAX. Most films were grown with an initial substrate temperature of 350°C followed by a final layer at 450°C. Some experimentation with lower initial substrate temperatures was carried out. A complete listing of all $CuInSe_2$ and subsequent CdS depositions is given in Appendices A through C.

During the early part of the year cells were completed with a few microns of CdS but it was subsequently shown that using layers of 1μm or less in thickness gave enhanced short circuit currents. This was shown by optical analysis to be directly due

to enhanced transmission through the CdS(2). Towards the end of the contract period CdS layers of about 1μm became standard.

2.2 Materials Analysis

Substrates are routinely analyzed using EDAX to ensure that no major change in layer composition has occurred. During the third quarter a recalibration of the IEC system was carried out with the cooperation of SERI. Seven IEC films were analyzed using wavelength dispersive x-ray spectrometry at SERI and the results of that analysis used to recalibrate the IEC system. In order to avoid progressive but unobserved degradation of the standards the seven films will be used in rotation to maintain calibration of the IEC system. Monitoring the performance of the IEC EDAX system with these standards over a number of months has shown that the error bands reported in the third quarterly report(4) are being well maintained.

Immediately following this report period, a sequence of high efficiency cells were made with most deposition runs yielding cells over 10%. Data from this sequence will be used to establish the composition range over which high efficiency cells can be made. Initial indications are that the range is of the order over a few atomic percent for each element, a result of considerable significance for ultimate commercial production.

As shown in Figure 3.18, Reference 1, the first $CuInSe_2$ layer and the composite layer are both highly textured as observed by SEM at >X2,000. However, this type of microscopy tends to disguise the existence of highly protuberant regions because of its large depth of field. In contrast, examination

under an optical microscope at high magnification is particularly sensitive to features rising significantly above the general film surface. In response to shorting problems with the tandem cells $CuInSe_2$ layers have been monitored in the optical microscope and it was found that many films which produced satisfactory single junction cells contained a population of small diameter but highly protuberant defects. These took the form of needles or spike-like growths of about 1μm in diameter but 3-5μm high at an areal density of ~ $10^5/cm^2$. A correlated study of specific areas in both the SEM and optical microscope was able to locate the defects. As would be expected normal SEM observation at low tilt angles, ~ 25°, generally failed to reveal their presence.

Figure 1 shows both a conventional SEM of a $CuInSe_2$ layer at 20° and also a high tilt angle stereo pair of a protuberant feature. The large tilt reveals the height of the feature (computed by stereoscopy to be 3•4μm high) and an associated void, presumably due to shadowing during the deposition. These defects are propagated through the subsequent CdS layer as shown by a high angle stereo pair of the surface of a $CdS/CuInSe_2$ cell (Figure 2) made on material deposited during the same run as Figure 1. It is evident that these defects are not impacting on the performance of single junction $CdS/CuInSe_2$ cells but they do have disastrous consequences on the yield of tandem cells made by depositing CdTe/CdS layers on this base.

2.3 Cell Analysis

A complete summary of cell data developed during the entire

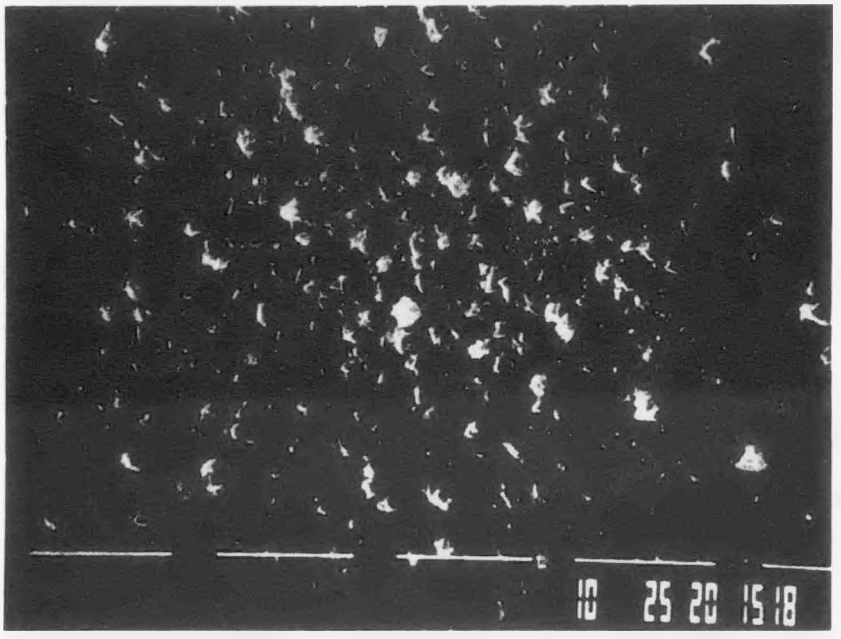

Figure 1a. $CuInSe_2$ substrate #31518.33.
Scanning electron micrograph at 20° tilt, x 2000

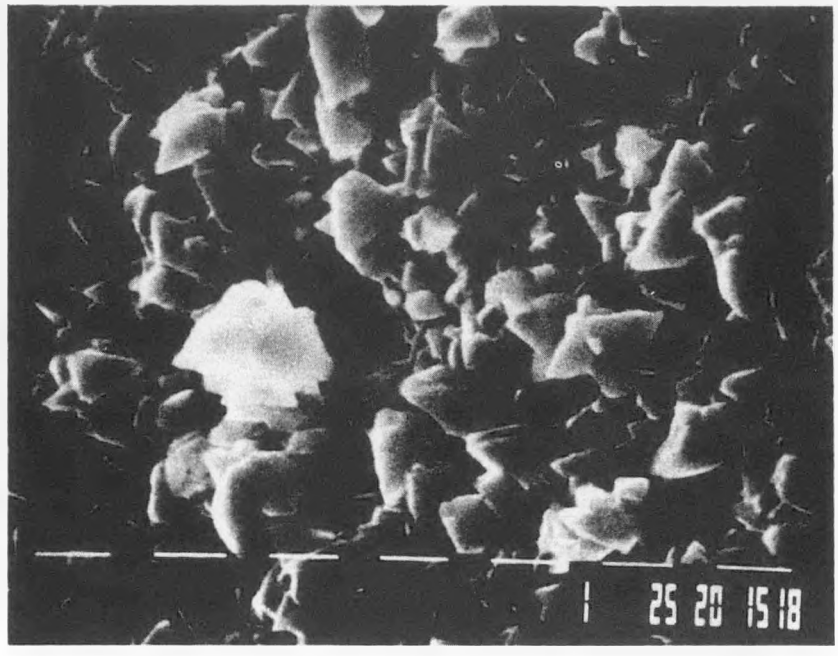

(b)

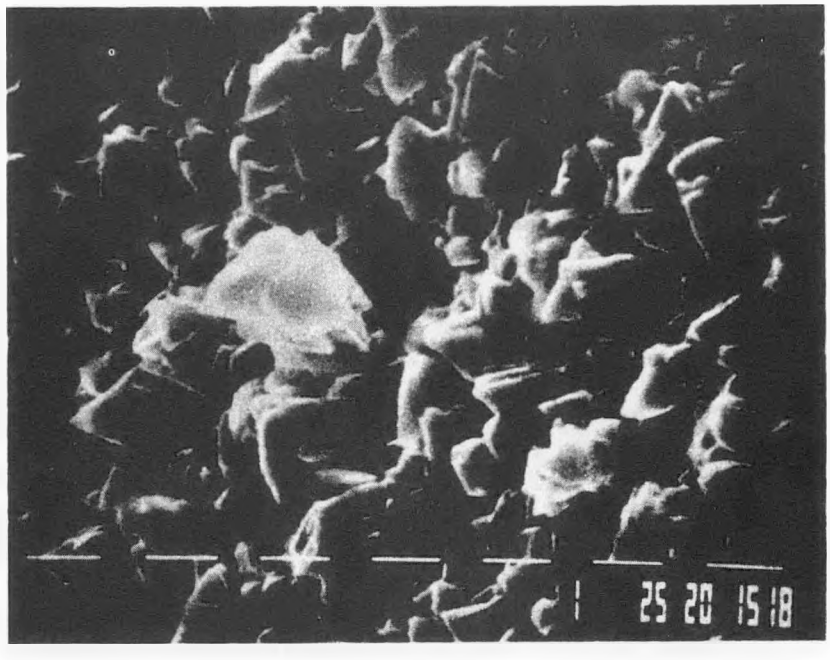

(c)

Figure 1 (cont'd). High tilt angle stereo pair at 10,000.
(b) left hand at 30°. (c) right hand at 45°.

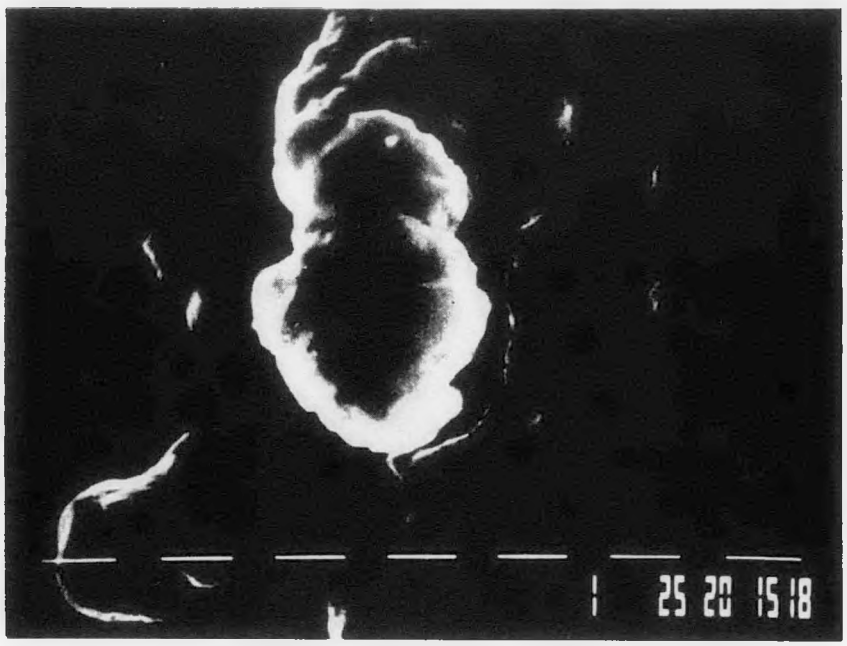

(a)

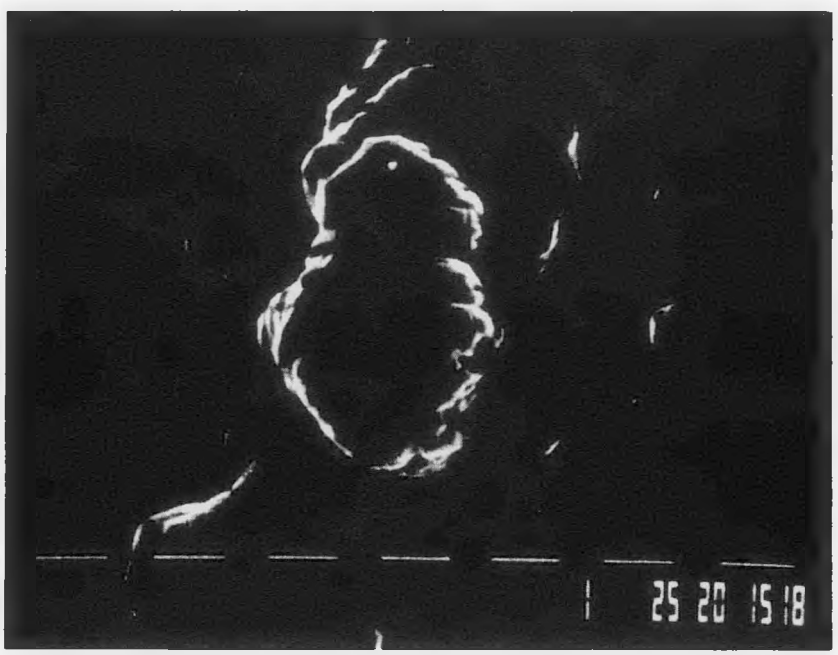

(b)

Figure 2. High angle stereo pair of the CdS film deposited on $CuInSe_2$ substrate #31518.11. (See Figure 1). (a) Left hand, tilt 30°. (b) Right hand, tilt 45°. x 10,000.

year is given in the appendices. Appendix D gives a convenient statistical analysis of results obtained from each substrate run.

As efficiencies improve, the sensitivity of the final cell performance to each step in cell construction will tend to rise. Towards the end of the year, the net sheet resistance of the thinner CdS and the ITO was becoming sufficient to reduce the achievable fill factor and hence the overall performance. Accordingly cells were made with two rather than one Ni contact tab and the resulting substantial improvement in maximum and average performance will be reported in the next quarter.

An operational test of the uniformity of the $CuInSe_2$ deposition process was performed by analyzing cells made on five substrates from a single deposition run. Table 1 gives the data from these tests and confirms very good uniformity of $CuInSe_2$ properties over the whole of the 3 x 3 matrix of substrates deposited in one evaporation.

Table 1

I-V parameters and standard deviations for 12 cells made on 5 substrates deposited during run #31493

Piece	Efficiency(%)	V_{oc}(V)	J_{sc}(mA/cm^2)	FF(%)
31493.23	8.72±0.31	.421±.002	31.3±0.3	58.8±1.9
.21	8.69±0.80	.410±.006	32.0±1.0	59.1±3.6
.11	7.98±0.41	.384±.008	31.7±0.7	59.0±1.0
.33	7.84±1.63	.376±.034	32.7±0.4	55.2±6.9
.22	9.25±0.26	.411±.003	34.0±0.6	59.7±1.0

The parameter contributing most of the spread appears to be fill factor. Short circuit current, which largely reflects the $CuInSe_2$ film quality shows a small spread indicating good

uniformity in the $CuInSe_2$ evaporator (the slightly higher J_{sc} for #31493.22 probably reflects the somewhat thinner CdS on those cells).

At the end of this report period, a major thrust was in progress to yield cells of over 10% efficiency. The experience gained with thinner CdS, close attention to the ITO deposition and the use of the two tab contacting did indeed produce cells over 10%. The data shown in Table 2 is for substrate 31537.21 which was made and tested during March 1985.

Table 2

Cell results for 12 cells made on substrate #31537.21
Tested 3/29/85

	V_{oc} (V)	J_{sc} (mA/cm^2)	FF (%)	Eff (%)
Max.	.405	34.30	66.00	10.28
Min.	.397	32.13	62.96	9.55
Mean	.401	33.29	65.13	9.95
Std.Dev.	.002	0.70	0.60	0.25

Subsequently, cells exceeding 10% efficiency were made on substrate 31505 that was deposited during this reporting period.

3. (CdZn)S/(CdHg)Te Cell Development

During the previous contract procedures were established for the production of CdS/CdTe cells as described in Appendix J(1), and modest efficiencies had been achieved of the order of 4%. Reasonable but not ideal contacting was achieved by depositing the CdTe on Mo/Cu for single junction cells and ITO/Cu for tandem devices. Some progress was made by depositing the CdTe in a partial pressure of O_2 but substantial further improvement was necessary to reach the efficiencies required for tandem devices. A further significant advance in efficiency was made during this contract period by the addition of small amounts of Hg during the CdTe deposition process. By the end of the contract year, the maximum efficiency achieved had been raised to 6.4%.

3.1 Film Growth

About 200 CdTe films have been grown during this reporting period. The deposition technique is essentially as described in Appendix J(1) but during the year some modifications were carried out in an attempt to improve the behavior of CdTe devices. The major thrust was directed to producing more strongly p-type films particularly in the region of the back contact. During the first part of the year a substantial number of films were deposited in a low background pressure of oxygen as preliminary results seemed to indicate some beneficial effects from this. Subsequently it was decided that no systematic benefit could be discerned and accordingly the practice was discontinued.

There are literature references to successful p-type doping

with P(5) and efforts were made to incorporate phosphorous during the film growth. A small furnace was mounted in one of the evaporator systems in order to thermally decompose a PH_3 flow. No beneficial effects on material properties or device performance were determined in these experiments and therefore the P doping trials were discontinued.

Experiments in which small amounts of Hg were incorporated into the CdTe films were however very encouraging and continue as a significant component of the ongoing research. The experimental arrangement to produce (CdHg)Te films has been described(4). The major observations on the growth and properties of (CdHg)Te films are as follows:

1) No Hg is incorporated into the films at substrate temperatures above 250°C.
2) The Hg content of a film is determined by the substrate temperature ($\leq$ 200°C) and is relatively insensitive to the Hg flux.
3) Hg suppresses the formation of free Te and single phase films can be produced down to substrate temperatures of 140°C. [The existance of Te precipitates in pure CdTe was described previously(5)].

Research in a parallel program #XL-4-03146-1(6) resulted in a model of the growth process in the presence of Hg which provides a rationale for the influence of Hg on the production of Te free films.

Substrate temperatures as low as 140°C proved unusable for devices as the high residual stresses in the films resulted in

separation from the substrate during device processing and most films are currently being deposited at 160°C.

3.2 Materials Analysis

The optical properties of the (CdHg)Te are routinely monitored using a Perkin-Elmer VIS/IR spectrometer; for a limited number of samples the band gap has also been derived from the spectral response behavior of CdS/(CdHg)Te devices. The correlation between (CdHg)Te composition and band gap published by Li(7) is used to estimate the actual Hg content of the film.

One pure CdTe film and four films containing Hg were analyzed at SERI using Auger electron spectroscopy. The results of these measurements are given in Table 3 and confirm that the Hg level in use is generally of the order of 5%.

Table 3

AES bulk compositions determined by SERI
Analysis #1040

Substrate	Hg(a/o)	Cd(a/o)	Te(a/o)
40127.22	0	51	49
40307.22	< 1	49.8	49.5
40321.13	4.2	46	49.8
40323.13	7.8	43.5	49.6
40327.13	4.6	45.7	48.7

The behavior of the thin Cu layer during the CdTe deposition and subsequent heat treatments has been reported previously. (2,3) These studies showed that CdTe deposited on thin Cu layers showed detectable Cu on the free top surface and a Cu-Te compound at the back contact. Previously reported observations were for CdTe deposit of substrate temperatures generally greater than

250°C. During this quarter some checks were made on CdTe deposited at low substrate temperatures which revealed generally similar behavior to that previously reported. Substrate #40311.31 was a (CdHg)Te film deposited at a substrate temperature of 160°C. AES revealed that Cu was again detectable on the front surface in the as-deposited film but a heat treatment of 3 hours at 300°C eliminated the Cu on the free surface although it was still detectable at the back contact. It should be noted that in general the Cu layer has been reduced in thickness to between 10 and 30 Å compared to the previous thickness of the order of 100 Å.

3.3 Cell Analysis

A complete compilation of data for film deposition and cell performance is given in Appendices E through H. A continuing obstacle to systematic cell optimization remains the extreme variability in device performance from run to run. The first major indication of an improvement in this area occurred when Hg was first introduced into the films during the third quarter of this contract year. Figure 3 shows the I-V curve of the best cell produced with a conversion efficiency of well over 6%. Five other deposition runs carried out at about that time yielded cells of over 5% efficiency. However following this period, a general decline of output was recorded with considerable variability from run-to-run.

During the final quarter of this contract, CdTe films were also being deposited under the parallel contract #XL-4-03146-1 using intentionally low growth rates at substrate temperatures

below 200°C. Some of the films produced were made into cells, one of which yielded the highest efficiency for CdTe without Hg. Figure 4 shows the I-V curve for this cell which is clearly being limited by a poor fill factor due to a blocking contact.

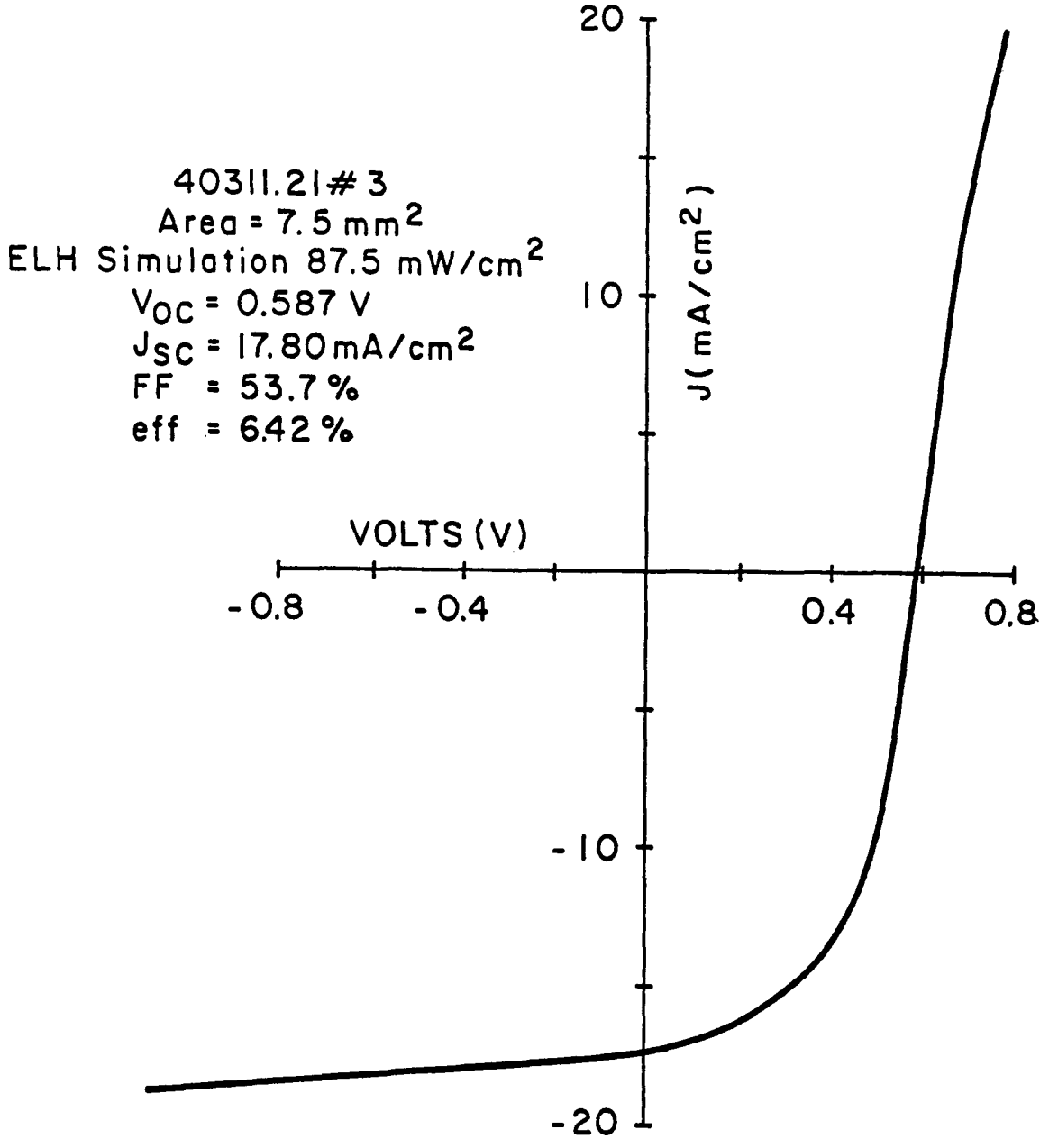

Figure 3. I-V curve for a CdS/(CdHg)Te solar cell containing ~ 5% Hg.

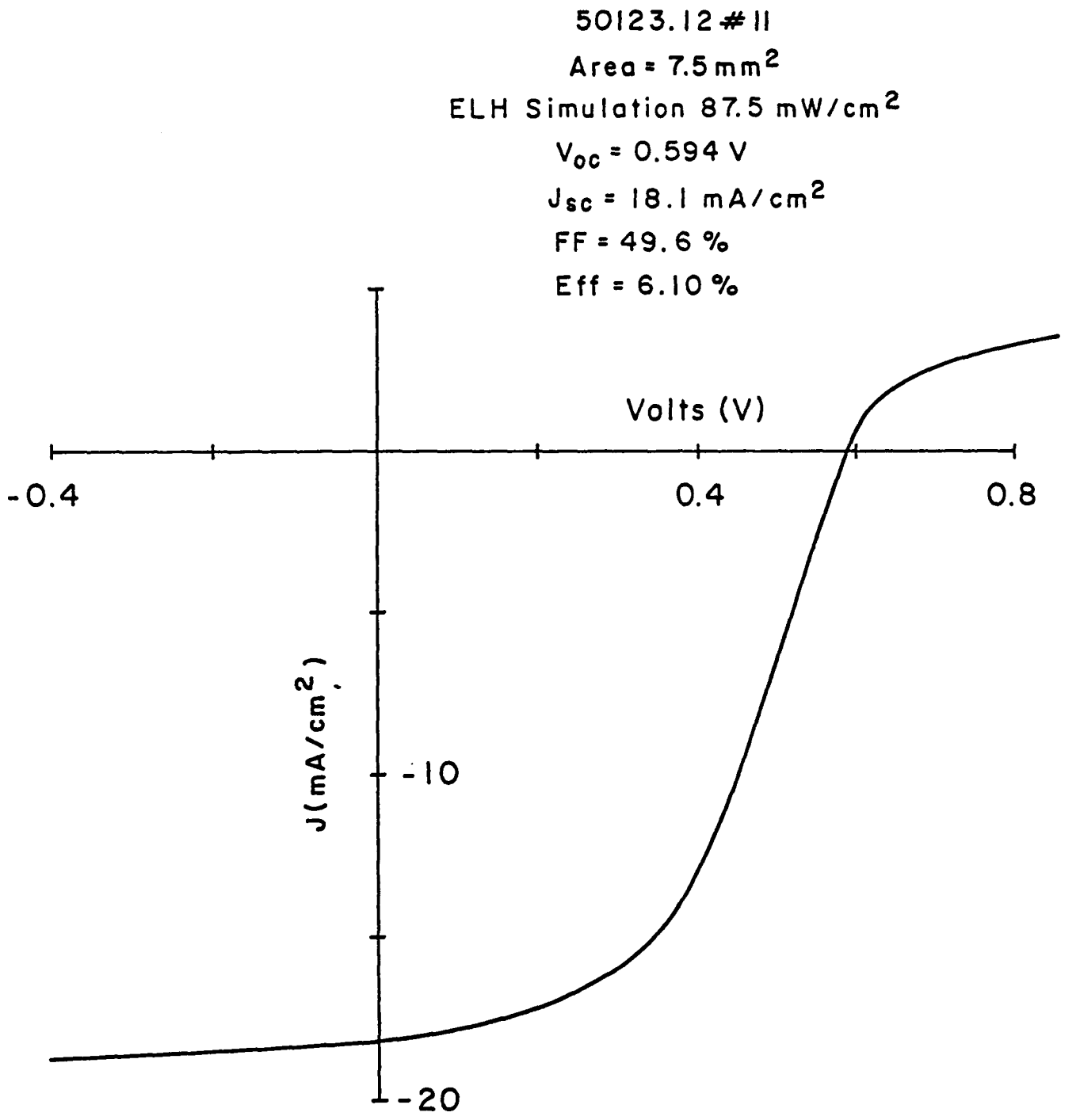

Figure 4. I-V curve for a CdTe/CdS cell. The CdTe was deposited at 180°C.

4. Tandem Cell Development

During this report period the first successful thin-film polycrystalline tandem cells were made. Efficiencies were generally low predominantly due to a contacting problem with the CdTe/CdS cell. During much of the contract period attention was focussed on improving the individual junctions and a relatively small number of tandem structures were actually manufactured. Progress on the CdS/CdTe cell has been the main obstacle to further tandem cell improvement.

4.1 Cell Processing

The tandem cells were produced by depositing the CdS/CdTe cell on top of an existing CdS/$CuInSe_2$ cell. The 1 x 1 inch 7059/Mo/$CuInSe_2$/CdS substrate layer is coated with an ITO layer followed by a 20-50 Å layer of Cu. (Ni bus bars are first deposited on the top surface of the CdS layer to provide a contact to the interconnect for individual cell testing). The CdTe layer is then deposited and heat treated, generally for two hours at 350°C. The device is completed by the deposition of about 1.5μm of undoped CdS followed by Ni bus bars and a final ITO layer.

An array of 12 tandem cells are delineated by a photolithography and etching process. A considerable amount of difficulty was encountered in trying to etch through the ITO interconnect layer. ITO layers which have not been heat treated etch readily in the cold HCl that is used for individual junction cell delineation. However, after the heat treatment given the

CdTe layer prior to the final CdS layer, it was shown that the ITO crystallizes and becomes much more resistant to HCl etching. A partially successful technique has been developed in which the ITO interlayer is connected to a Zn electrode during the HCl etching process. The resulting galvanic effect considerably enhances the etching rate.

4.2 Materials Analysis

During the major portion of this reporting period tandem cell production was on hold while improvements were made to the individual junction cells. Towards the end of the contract period as the CdS/$CuInSe_2$ cell performance routinely exceeded 10%, a series of tandem cells were produced. It was at this time that problems were encountered with the protuberances from the $CuInSe_2$ layer described in Section 2.2. Most tandem devices were found to be shorted and optical and SEM examination revealed that preferential etching down the protuberances was causing the shorting behavior. At the end of the contract period, the initial $CuInSe_2$ layer was deposited at a reduced temperature and this was yielding smoother $CuInSe_2$ layers. Those experiments are still in progress.

4.3 Cell Analysis

A complete listing of tandem production and device results is given in Appendices I and J. Figure 5 shows the current-voltage curve for a tandem device made with a (CdHg)Te cell containing about 7% Hg. The maximum short circuit current achieved through the tandem device is about 10mA/cm^2 and the

highest open circuit voltage is about 1 V. The major efficiency limiting factor is the behavior of the CdS/CdTe cell and improvements in this component of the tandem will be immediately reflected in overall tandem performance.

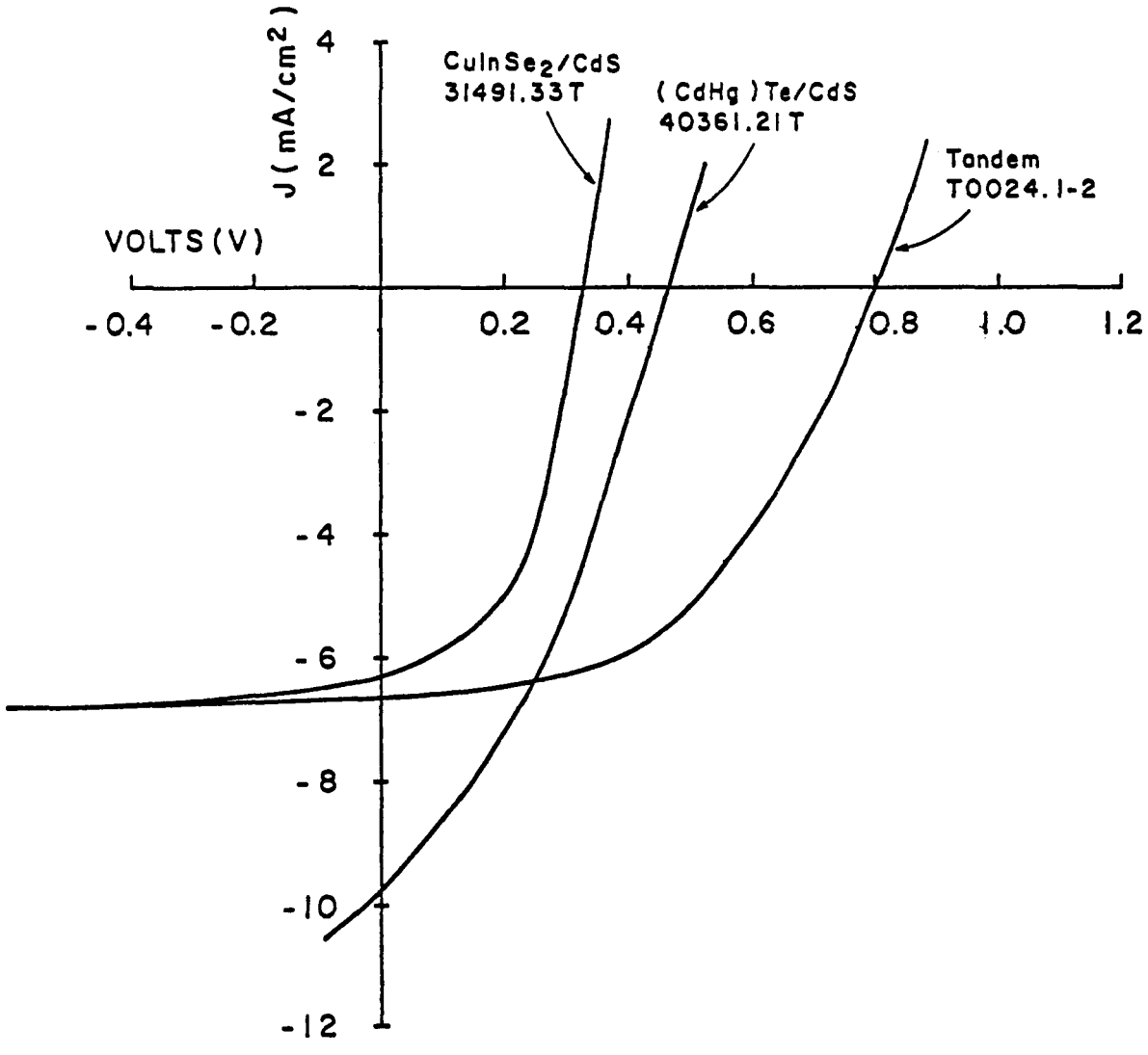

Figure 5. I-V curves for tandem cell and the individual junctions. ELH simulation 87.5 mW/cm^2.

5. Conclusions

- A process has been developed that reproducibly yields $CuInSe_2$/CdS cells of over 10% efficiency.
- The addition of small concentrations of Hg to CdTe has improved the reproducibility and lowered the spread in performance of CdTe/CdS cells.
- Monolithic CdTe/CdS|$CuInSe_2$/CdS tandem cells can be produced by a sequential deposition process.
- Improvements in the CdTe/CdS junction will be immediately reflected in the performance of the thin-film tandem cell.

6. References

1. IEC Final Report, #XL-3-03065-1, July 1984.
2. IEC First Quarterly Report, #XL-4-04025-1, August 1984.
3. IEC Semi-Annual Report, #XL-4-04025-1, November 1984.
4. IEC Third Quarterly Report, #XL-4-04025-1, February 1985.
5. IEC Semi-Annual Report, #XL-3-03065-1, November 1983.
6. IEC Final Report, #XL-4-03146-1, July 1985.
7. T.P.L. Li, Proceedings IEEE 33rd Electronic Components Conference, 546-551, 1983.

7. Contributors

The following members of IEC contributed to the research during this period.

D. R. Ahrens, E. G. Ashmead, S. K. Buchanan, A. S. Canedo, J. M. Cebulka, L. C. DiNetta, R. D. Dozier, C. T. Field, S. I. Gordon, J. E. Hall, S. S. Hegedus, T. B. Kinaman, T. W. Kottke, P. G. Lasswell, P. H. Mauk, B. E. McCandless, K. E. Schubert, J. R. Smith, S. L. Spinner, G. B. Streetman, H. O. Wardell, and J. R. Wheeler.

APPENDIX K

$CuInSe_2$/CdS-CdTe/CdS Polycrystalline Tandem Solar Cells

R.W. Birkmire, L.C. DiNetta, J.D. Meakin, J.E. Phillips

$CuInSe_2$/CdS-CdTe/CdS POLYCRYSTALLINE TANDEM SOLAR CELLS

R. W. Birkmire, L. C. DiNetta, J. D. Meakin, J. E. Phillips

Institute of Energy Conversion
University of Delaware
Newark, Delaware 19716

ABSTRACT

monolithic optically and electrically coupled ndem junction has been produced. The component lls are $CuInSe_2$/CdS and CdTe/CdS polycrystalline terojunctions. A 3% efficient device with over 0 volt open circuit voltage and 6 mA/cm^2 short rcuit current has been achieved. It is esti-ted that an efficiency of over 20% should be actically achievable.

INTRODUCTION

ffective low cost power generation using photo-oltaic modules requires solar cells with high nversion efficiencies[1]. The most promising proach to obtain major improvements in cell fficiency is the use of multijunction cell tructures[2,3]. To date, the major emphasis in ultijunction cells has focused on single rystal III-V materials[4] and thin films based on morphous-Si[5]. In this paper we report on a hin-film polycrystalline $CuInSe_2$/CdS-CdTe/CdS andem heterojunction solar cell. The $CuInSe_2$/CdS and CdTe/CdS cells used as the consti-uent cells since each has proven efficiency over 0%[6,7] and their bandgaps are appropriately tched for a tandem structure.

APPROACH

nalysis of the tandem structure based on experi-ental results showed that a practical efficiency f over 20% should be achievable. (CdZn)S was sed as the window material in the calculation to ssess the optimum V_{oc}. Table 1 summarizes the esults of the calculations for the individual and andem cells. Both heterojunctions were assumed o be dominated by interface recombination with an nterface recombination rate of 3×10^7 cm/sec. A 0% loss due to front surface reflection and con-acting was used for all calculations. The quan-um efficiency was assumed to be 100% for the $CuInSe_2$ cell and 80% for the CdTe cell. In the andem structure the value was reduced to 90% for he $CuInSe_2$. Using the same assumptions but CdS s the window material yielded individual cell esults comparable to the experimental values re-orted for $CuInSe_2$[6] and CdTe[7] cells.

PREPARATION

Figure 1 shows a cross section of the tandem cell structure. The $CuInSe_2$ is deposited from the elements and the CdTe and CdS from compound powder sources. The $CuInSe_2$ cell is similar in structure to the 10.6% cell reported by Boeing[6]. The CdTe is grown at a substrate temperature of 300°C with an oxygen over pressure in the vacuum system. Prior to the CdS deposition, the CdTe film is heat treated in air at 300°C for 3 hours. An undoped layer of CdS is deposited to form the hetero-junction followed by a heavily In doped CdS layer.

STRUCTURE

To make a monolithic tandem structure requires a tunnel junction, grid structure or transparent metal to provide a transparent ohmic contact be-tween the cells. ITO was used as the ohmic contact to the CdS and, by depositing a 100 A of Cu between the ITO and CdTe, a reasonable contact to the CdTe is formed. The cell area and contacts are defined by a photolithography-etching procedure which yields 12 tandem cells each 3x3 mm^2 on a 2.5x2.5 cm^2 substrate. The cell has three termi-nals so the individual and tandem cell character-istics (J-V, spectral response, etc.) can be measured.

RESULTS

The J-V characteristic of the highest efficiency tandem cell is shown in Figure 2 along with the J-V characteristics of the individual cells. Table 2 is a summary of the cell parameters. The V_{oc} of the tandem is over 1.0 volt and the efficiency is over 3%.

SUMMARY

The $CuInSe_2$/CdS-CdTe/CdS device demonstrates that a two cell multi-bandgap tandem structure can be made from single junction polycrystalline thin-film solar cells. Care must be taken to provide a transparent ohmic interconnect between the two cells and to ensure that the process for making the second device does not adversely affect the initial cell. Within these restrictions it should be possible to build thin-film polycrystalline tandem devices with a substantially higher efficiency than their single junction counterparts.

Presented at the 17th IEEE Photovoltaic Specialists Conference, Orlando, Florida, May 1-4, 1984

APPENDIX L

Material Requirements For High Efficiency $CuInSe_2/CdS$ Solar Cells

R.W. Birkmire, R.B. Hall, J.E. Phillips

MATERIAL REQUIREMENTS FOR HIGH EFFICIENCY $CuInSe_2$/CdS SOLAR CELLS

R. W. Birkmire, R. B. Hall, J. E. Phillips

Institute of Energy Conversion
University of Delaware
Newark, Delaware 19716

ABSTRACT

$CuInSe_2$/CdS solar cells with efficiencies greater than 8% have been made by the elemental evaporation of $CuInSe_2$ onto Pt and Mo contacts. Both Pt and Mo can give I-V characteristics which show a 'second diode blocking contact' in the completed cell. The 'second diode' behavior does not appear to affect the final defice efficiency.

In-doped high conductivity CdS was usually evaporated onto the $CuInSe_2$ to make the final device. High conductivity CdS was used to ensure that most of the depletion layer would be in the $CuInSe_2$ thereby aiding in the collection of minority carriers and giving a diode quality factor close to unity. Other devices have been made over a range of CdS conductivities in order to increase our understanding of junction behavior.

INTRODUCTION

The properties of $CuInSe_2$ dictate the device design for high efficiency heterojunction solar cells. The $CuInSe_2$ must be p-type to use CdS as the window material. To limit interface recombination a field of about 10^5 V/cm at J_{sc} is optimum since a much higher field would result in a lower barrier height. This sets an upper limit of the $CuInSe_2$ conductivity of about 1.0 to 10 Ω^{-1} cm^{-1}. To insure high V_{oc}, the Fermi level should be less than 0.1 eV above the valence band thus setting a lower bound of 10^{-2} Ω^{-1} cm^{-1} on the $CuInSe_2$ conductivity. $CuInSe_2$ films with these properties have been deposited by physical vapor deposition from elemental effusion sources. Substrate temperatures from 250-450°C have been used.

To provide ohmic contact to the $CuInSe_2$, a material that can withstand the high substrate temperatures and the "corrosive" atmosphere during deposition is needed. Mo which has been used by Boeing(1) and Pt both appear to satisfy these criteria. Au and Ni appear to interact with the $CuInSe_2$ during deposition resulting in low J_{sc} and generally poor device performance.

To form the heterojunction, the CdS conductivity must be high enough so that the diode A-factor is less than about 1.1 and the Fermi level is close to the conduction band to maintain a high V_{oc}. CdS with conductivities of 1 to $10^{+3}\Omega^{-1}cm^{-1}$ are easily obtained using indium doping. The upper limit of the conductivity is dictated by a loss of transmission through the CdS at high indium doping levels.

Devices have been made with a range of conductivities in order to increase our understanding of junction behavior. By varying the ratio of the conductivities of the CdS and $CuInSe_2$, it is possible to vary the width of the depletion region in the $CuInSe_2$. The resulting changes in J_{sc} and spectral response show that the current collected from the $CuInSe_2$ is enhanced by field collection in the depletion region. If the CdS is made highly resistive and photoconductive, the cells have a light to dark crossover in the I-V characteristics. These effects of the photoconductive CdS controlling the response of the active semiconductor are analogous to those of Cu_2S/CdS devices(2-4).

DEVICE PREPARATION

Devices were made on either 7059 glass or alumina slides sputter coated with Mo (thickness > 1 μm). On some samples 500Å of Pt was added by e-beam evaporation. Two-layer $CuInSe_2$ films made with the same substrate temperature conditions and elemental composition as Boeing(1) were evaporated in an effusion source system. The source temperatures are used to control the deposition conditions rather than controlling the fluxes as in the Boeing system. Figure 1 is a schematic of the effusion source system which consists of three source bottles and a standard substrate heater assembly. The temperature of the source liquids must be controlled to ± 1°C in order to reproducibly control the stoichiometry and resistivity of the $CuInSe_2$ films.

After the $CuInSe_2$ evaporation, In and CdS were simultaneously evaporated onto the substrate in a separate system to provide the high conductivity CdS layer. The top contact to the CdS consists of a transparent ITO film and a Ni bus bar which provides a robust contact for cell testing.

A device structure has been used to make $CuInSe_2$/CdS cells which consist of twelve 3x3 mm^2 cells made on a 2.5x2.5 cm^2 sample (Figure 2). The cell areas are delineated by a photolithographic-etch process (see Figure 3). With this configuration of cells, the uniformity of the $CuInSe_2$

Presented at the 17th IEEE Photovoltaic Specialists Conference, Orlando, Florida, May 1-4, 1984

substrate is directly evaluated by the device performance. Additionally, samples can be sectioned into individual cells to evaluate the effects of different heat treatments on identical cells.

RESULTS

CdS Resistivity

The effect of CdS resistivity on the photoresponse of CdS/$CuInSe_2$ thin-film heterojunction solar cells has been examined. We conclude that devices in which trapping at deep levels in the photoconductive CdS dominates the junction characteristics (2-4). Many similarities between the two types of devices have been noted, such as a large crossover between light and dark I-V curves (Figure 4), enhancement of the long wavelength spectral response by bias light (Figure 5), and spectrally dependent enhancement and quenching of the capacitance (Figure 6). These effects are absent with low resistivity (non-photoconductive) CdS. These results are consistent with the interface collection model in which the field at the heterojunction controls interface recombination (4-5). On optimized, high efficiency $CuInSe_2$/CdS solar cells the photoresponse is much less sensitive to light bias indicating reduced interface recombination.

I-V RESPONSE

Many times the I-V characteristic of a $CuInSe_2$/CdS cell will bend over in forward bias indicating a second diode in the device. This type of blocking response in shown in Figures 7 and 8. The second diode behavior occurs with both the Pt and Mo back contacts and does not limit the final efficiency of the devices shown. Devices whose efficiencies are greater than 8% have also been made with material that does not show the blocking response (Figure 9).

Since the occurrence of the second diode is independent of the type of back contact, resistivity of the CdS, and light intensity, it is probably due to inhomogeneities in the $CuInSe_2$ layer. EBIC scans across $CuInSe_2$/CdS cell cross sections support this conclusion (6).

SUMMARY

$CuInSe_2$/CdS cells of efficiencies greater than 8% have been made on both Mo and Pt contacts. These devices are made with low resistivity In-doped CdS. The initial I-V characteristics of the high efficiency devices can show a blocking diode behavior which does not appear to affect the final device characteristics. $CuInSe_2$ cells made with high resistivity CdS exhibit device behavior completely analogous to Cu_2S/CdS devices where the response is dominated by the photoconductive CdS.

ACKNOWLEDGEMENTS

We wish to acknowledge the efforts and contribution of the entire research staff at the Institute of Energy Conversion. This work was supported by a contract from the Department of Energy administered by the Solar Energy Research Institute.

REFERENCES

1. R. A. Mickelsen, W. S. Chen, "High Photocurrent Polycrystalline Thin-Film CdS/$CuInSe_2$ Solar Cell", Appl. Phys. Lett., 36, 371 (1980).
2. P. F. Lindquist and R. H. Bube, "Photocapacitance Effects of a CdS/$CuInSe_2$ Heterojunction", J. Appl. Phys., 43, 2839 (1972).
3. A. F. Fahrenbruch and R. H. Bube, "Heat Treatment Effects in Cu_2S/CdS Heterojunction Photovoltaic Cells", J. Appl. Phys., 45, 1264 (1974).
4. A. Rothwarf, "The CdS/Cu_2S Solar Cell: Basic Operation and Anomalous Effects", Solar Cells, 2, 115 (1980).
5. A. Rothwarf, J. Phillips and N. C. Wyeth, "Junction Field Recombination Phenomena in the CdS/Cu_2S Cell", Proc. 13th IEEE Photovoltaic Specialists Conference, 399 (1978).
6. P. E. Russell, O. Jamjoum, R. K. Ahrenkiel and L. L. Kazmerski, "Properties of the Mo-$CuInSe_2$ Interface", Appl. Phys. Lett., 40, 995 (1982).

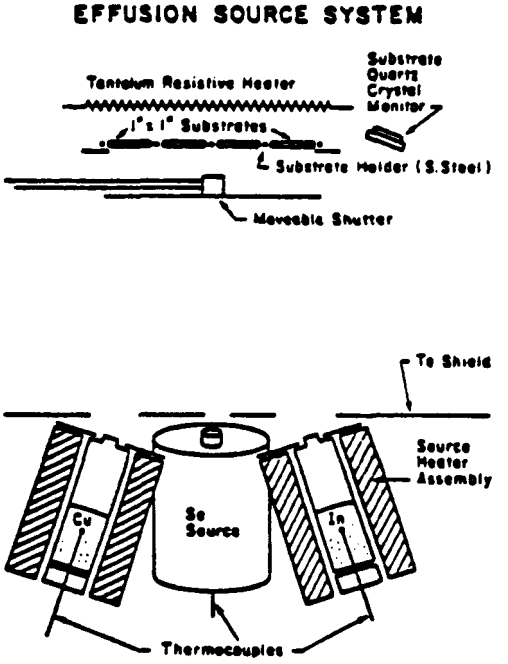

Figure 1. $CuInSe_2$ evaporation system.

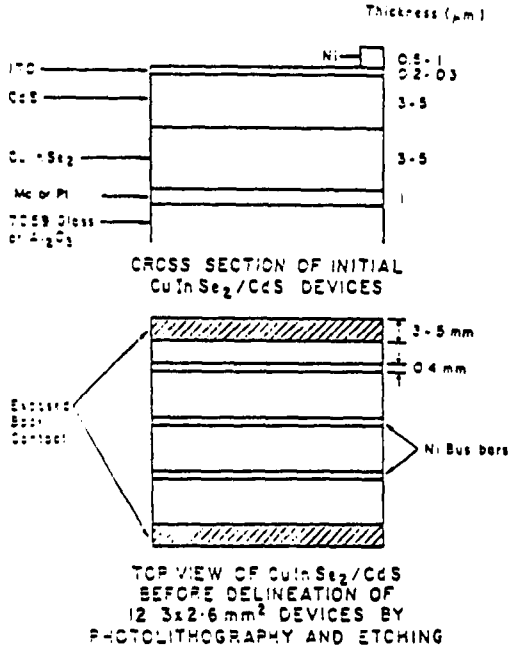

Figure 2. $CuInSe_2/CdS$ sample before delineation of individual cells.

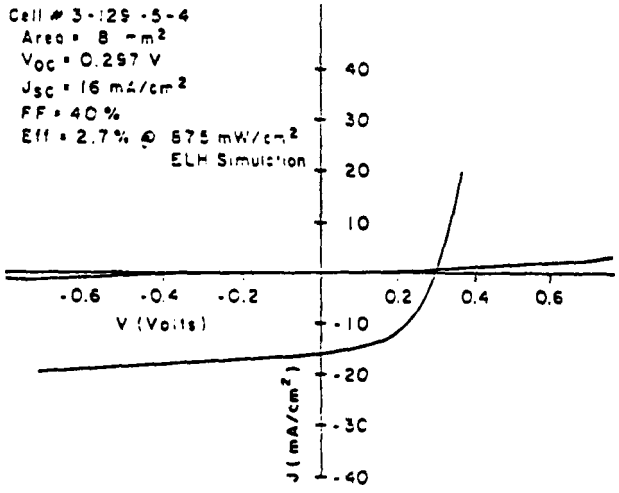

Figure 4. J-V characteristics of $CuInSe_2/CdS$ cell made with high resistivity CdS showing light to dark crossover.

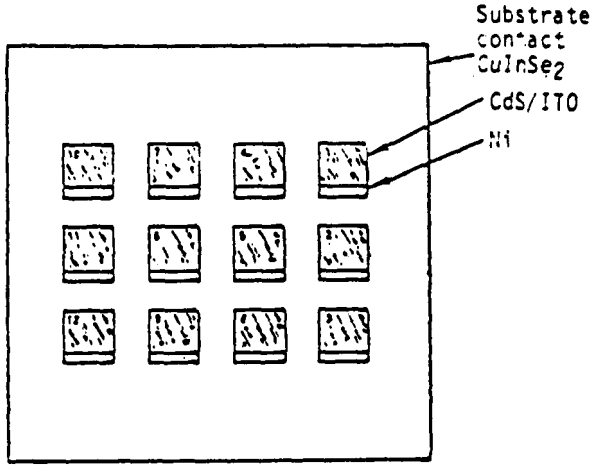

Figure 3. Final $CuInSe_2/CdS$ configuration.

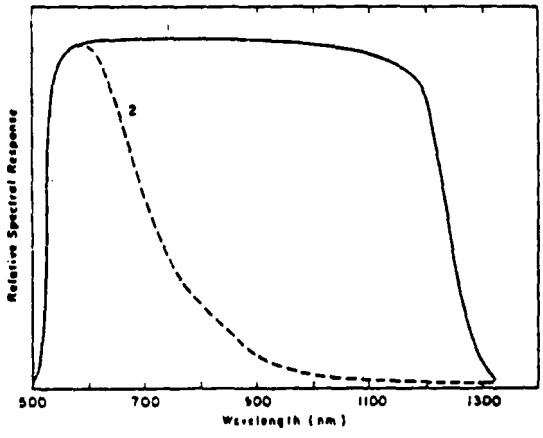

Figure 5. Relative spectral response of $CuInSe_2/CdS$ solar cells:

Curve 1: Low resistivity CdS with and without light bias; high resistivity with light bias.

Curve 2: High resistivity without light bias.

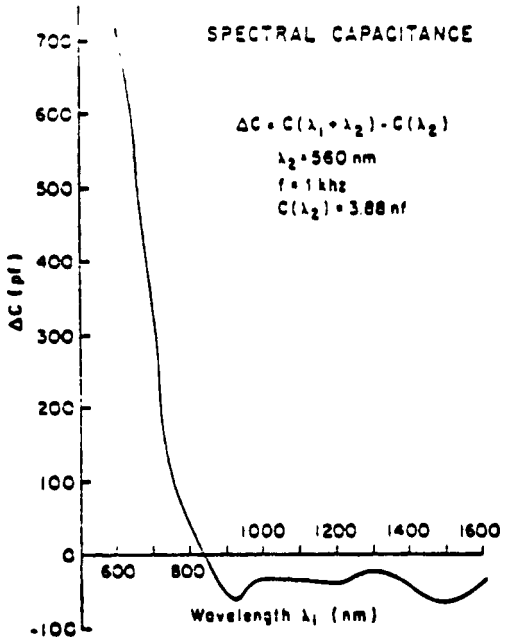

Figure 6. Spectral capacitance of high resistivity and photoconductive CdS showing enhancement and quenching effects.

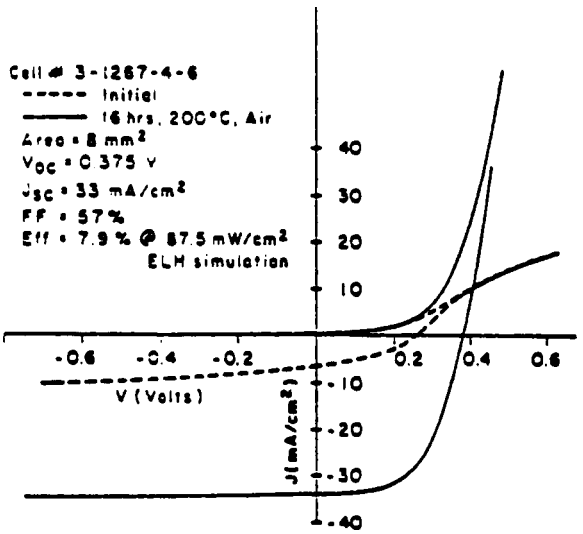

Figure 7. J-V characteristics of high efficiency Mo-$CuInSe_2$/CdS cells with "second diode blocking behavior."

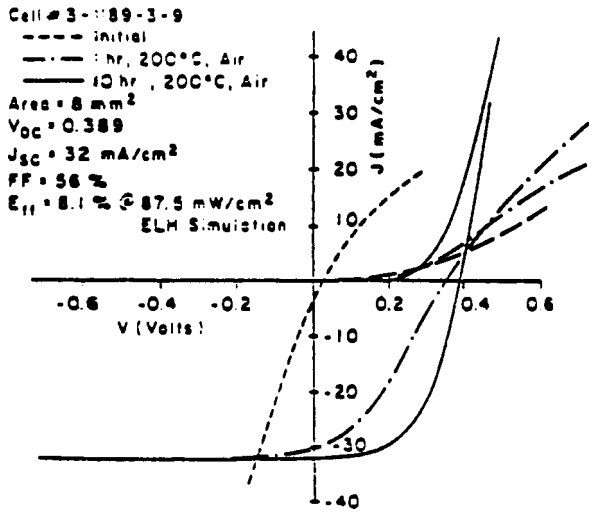

Figure 8. J-V characteristics of high efficiency Pt-$CuInSe_2$/CdS cells with "second diode blocking behavior".

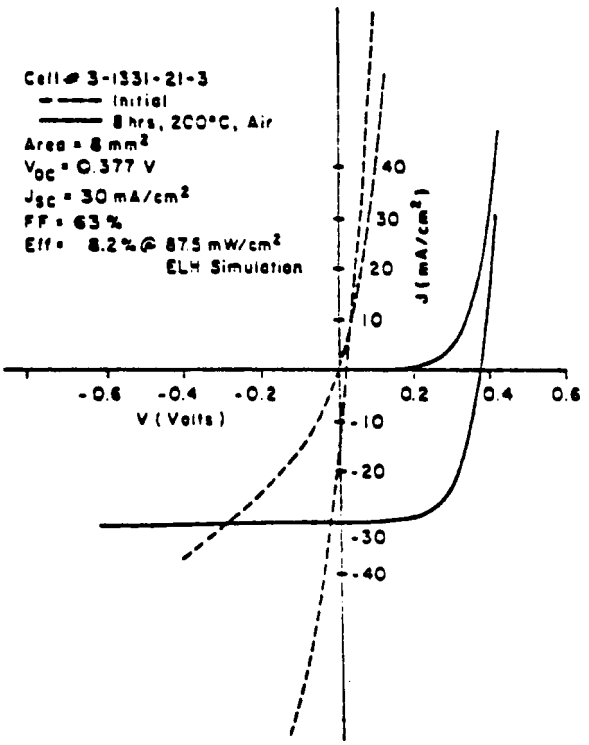

Figure 9. J-V characteristics of high efficiency Mo-$CuInSe_2$/CdS cells without "second diode blocking behavior".

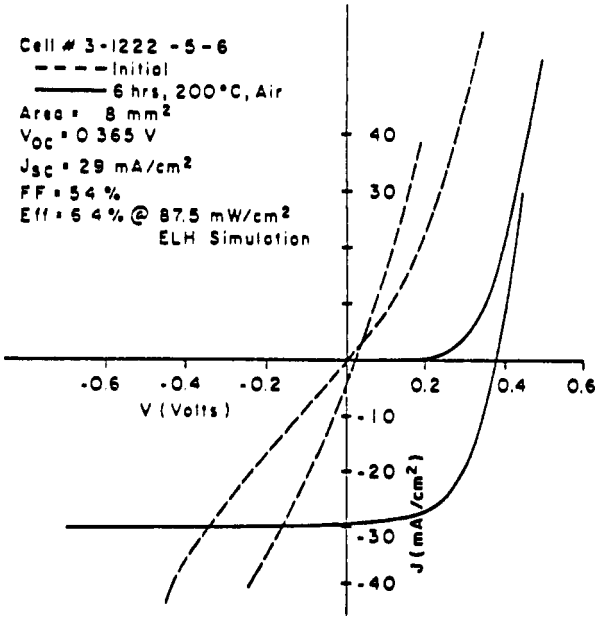

Figure 10. J-V characteristics of high efficiency Pt-$CuInSe_2$/CdS cells without "second diode blocking behavior".

APPENDIX M

Thin-Film Tandem Solar Cells

J.E. Phillips, R.W. Birkmire, L.C. DiNetta, J.D. Meakin

THIN-FILM TANDEM SOLAR CELLS

J. E. Phillips, R. W. Birkmire, L. C. DiNetta, J. D. Meakin

Institute of Energy Conversion
University of Delaware
Newark, Delaware 19716

ABSTRACT

A monolithic optically and electrically coupled tandem solar cell has been made with polycrystalline thin-film materials. The component cells are CdS/CdTe and CdS/$CuInSe_2$ heterojunctions made by physical vapor deposition. To date, a device of 3% efficiency with an open circuit voltage over 1 volt and a short circuit current of 6 mA/cm^2 at 87 mW/cm^2 has been made. The efficiency has been limited primarily by difficulties in making an ohmic transparent contact to the CdTe at the tandem cell interconnect. It is estimated that efficiencies of 17% are practically achievable with CdS, and efficiencies of over 20% are possible with (CdZn)S.

INTRODUCTION

Effective low-cost power generation using photovoltaic modules requires solar cells that have high conversion efficiencies and can be mass produced at low-cost. Recent studies(1) have indicated that a minimum flat plate module efficiency of near 15% at air mass one will be necessary to satisfy this goal. In order to produce modules of 15% efficiency, the solar cells must have an efficiency of 16 to 17% to compensate for interconnect and shading losses.

A single junction solar cell can only utilize photons of energy exceeding the bandgaps of the absorbing semiconductor. This and other losses puts a thermodynamic limit on the maximum efficiency of a single junction device under unconcentrated sunlight of about 30%(2). Raising the concentration ratio to its terrestrial maximum of 45,900 suns increases the efficiency limit to 40%(2).

By positioning a second solar cell of smaller bandgap to intercept the lower energy photons which pass through a wider bandgap solar cell, the total conversion efficiency can be increased. With an infinite stack of these junctions, the thermodynamic limit is 86.8% under 45,900 suns concentration and 68.2% under unconcentrated sunlight(2). Tables 1 and 2 show the limits for finite structures of these devices.

The increase in complexity of device manufacture weighed against

Presented at the 166th Electrochemical Society Meeting, New Orleans, October 1984

the increase in efficiency practically limits the number of cells in a multijunction device to 2 at present(3). Two cell tandem systems can either be electrically connected in series (two terminal) or electrically isolated (four terminal). The maximum efficiency of these tandem structures are between 36% and 37% under AM1 insolation(3). To date, major emphasis in tandem cells has focussed on single crystal III-V materials(4) and thin-films based on amorphous Si:H(5). Only recently has there been work on polycrystalline thin-film materials(6,7). Since all of the high efficiency polycrystalline thin-film devices (efficiencies >10%) have been based on CdS or (CdZn)S as a window material, design studies of cells based on these window materials have been carried out(8). The maximum efficiencies at AM1 computed for two junction tandem devices are 21% for CdS based materials and 26% for (CdZn)S based materials.

In this paper we report on the development of a thin-film polycrystalline CdS/CdTe-CdS/$CuInSe_2$ tandem heterojunction cell. The CdS/CdTe and CdS/$CuInSe_2$ cells were used as the constituents of the tandem device since their bandgaps are close to optimum and both have a proven efficiency over 10%(9,10).

APPROACH

Practical efficiency limits for polycrystalline thin-film tandem cells will necessarily be lower than the idealized cases calculated previously. In order to assess the potential for further improvement, an analysis of the practical achievable performance parameters has been made. The maximum achievable current for 100 mW/cm^2 normal insolation has been computed using an AM-1.5 direct insolation spectrum(11).

$CuInSe_2$

The maximum achievable current with a window of CdS (Eg = 2.4 eV) assuming 100% quantum efficiency is 42 mA/cm^2. For (CdZn)S of 2.6 eV bandgap (~ 30% Zn), the current is 44 mA/cm^2. If a 10% loss due to front surface reflection, gridding, etc. is assumed, the practical limit is computed to be 38 and 40 mA/cm^2 respectively.

It is reasonably certain that the heterojunctions with CdS are dominated by interface recombination. If we assume that the electron affinity mismatch, ΔE_c, between $CuInSe_2$ and CdS is 0.2 eV, the interface recombination rate, S_I, is 3×10^7 cm/sec and the Fermi level is 0.05 eV above the $CuInSe_2$ valence band, an open circuit voltage of ~ 0.4 V is expected. Making the assumption that changing the electron affinity match by using (CdZn)S will be directly reflected in V_{OC}, one could expect ~ 0.6 V for an optimum cell. This range of open circuit voltages coupled with the field dependent current collection which is believed to be operating will limit the fill factors to about 65% resulting in the efficiencies shown in Tables 3 and 4.

In conclusion it is seen that there may be scope for some further

improvement in a $CuInSe_2$/(CdZn)S cell but there is no firm basis for expecting efficiencies to significantly exceed ~ 15%.

CdTe

Computations for CdTe/CdS were carried out with the same assumptions as for $CuInSe_2$/CdS namely ΔE_c = 0.2 eV, S_I = $3x10^7$ cm/sec. A collection efficiency of 80% is assumed for the CdTe case because of the lower absorption coefficient. The results are given in Table 3. The fill factors are higher to reflect the significant increase in open circuit voltage. As with the $CuInSe_2$ calculation, it is assumed that the reverse saturation current and therefore V_{oc} is controlled by recombination at the interface. Hence, removing the electron affinity mismatch of almost 0.2 eV, would give a similar increase in open circuit voltage. The results are given in Table 4 for (CdZn)S.

Tandem

Whatever the ultimate efficiency limit of a single junction polycrystalline cell, there will be a very significant increase if successful tandem junctions can be made. For a current coupled tandem cell based on $CuInSe_2$ and CdTe heterojunctions, the J_{sc} will be set by the $CuInSe_2$/CdS junction at ~ 18 mA/cm^2 (90% quantum efficiency). Hence, we conclude that the efficiencies of 17% for CdS and 21% for (CdZn)S based tandem cells as shown in Tables 3 and 4 should be achievable.

DEVICE DESIGN AND PREPARATION

Although the efficiency limits have been discussed, little attention has been paid to the practical design features involved in making a monolithic tandem cell. Two major considerations that need to be addressed are; 1) the type of interconnect between the cells, and 2) the effects of the fabrication steps on the individual cell properties.

There are several ways to provide a transparent ohmic contact between the two cells. If a tunnel junction interconnect is used, the CdS and CdTe films must be highly conducting at the interface between the two cells. Since the properties of these films required at the heterojunctions will, in general, be different than at the tunnel junction, precise control of the film properties during deposition is needed. Another approach to interconnecting the cells is a transparent metal or grid structure which places less stringent requirements on the CdS and CdTe film properties. However, the interconnect must make ohmic contact to p-type CdTe and n-type CdS and have a transmission of at least 90% so that the loss in light generated current due to the interconnect is less than 10%. We have used ITO to make ohmic contact to the CdS and found that a 100 A layer of Cu between the ITO and CdTe forms a reasonable contact to the CdTe. The copper is a p-type dopant in CdTe and is believed to be incorporated in the CdTe film during

deposition modifying at least the contact region of the film. Bonnet(12) has previously reported the use of copper to improve the contact to CdTe.

In the actual making of tandem devices, care must be taken so that the process for making the second device does not adversely affect the initial cell. In depositing the CdTe film on the $CuInSe_2$ cell, the lowest satisfactory substrate temperature (300°C) was used at first to minimize the thermal effect on the $CuInSe_2$ cell. However, we found that the $CuInSe_2$ cell was not as sensitive to temperature as initially expected and have made tandem cells with CdTe films grown at as high as 400°C.

Figure 1 shows a cross-section of the tandem cell structure. The $CuInSe_2$ film is deposited on a Corning 7059 glass slide sputter coated with approximately 1 μm of Mo. The $CuInSe_2$ deposition system consists of three elemental source bottles where precise temperature control of the molten Cu, In and Se is used to control the effusion rates and thus the film composition. The $CuInSe_2$ film is grown in two stages in a manner similar to Mickelsen and Chen(13), where initially a copper rich film (composition typically 26% Cu, 24% In and 50% Se) is grown at a substrate temperature of 350°C followed by an indium rich film (composition typically 20% Cu, 28% In, 52% Se) deposited at 450°C. The composition of the composite film is typically 25% Cu, 25% In and 50% Se. The average growth rate of the $CuInSe_2$ film is typically 10 Å/sec.

The CdS and CdTe are both deposited from compound source bottles where the effusion rate again is controlled by precisely controlling the source temperature. In the CdS system, there is an indium source bottle used to dope the films and typically, the CdS is deposited at a growth rate of 0.3 μm/min at a substrate temperature of 200°C.

A 3 to 5 μm In doped CdS layer with a resistivity of nominally 0.01 Ω-cm is deposited to form the $CdS/CuInSe_2$ junction. The low resistivity CdS film insures that the depletion layer is entirely in the $CuInSe_2$. A sputtered ITO film 2500 Å thick and a Ni bus bar are deposited to provide a top contact to the $CdS/CuInSe_2$ cell followed by 100 Å of Cu as described above.

The CdTe is deposited at a growth rate of 0.1 to 0.3 μm/min and substrate temperatures from 300°C to 400°C with an oxygen over pressure in the vacuum system. Prior to the CdS deposition the CdTe film is heat treated at 300°C for 3 hours in air. An undoped layer of CdS (~ 0.5 μm) is deposited to form the CdS/CdTe junction followed by an In doped CdS layer. The undoped CdS is used at the interface to prevent indium, an n-type dopant in CdTe, from diffusing into the CdTe. A sputtered ITO film 2500 Å thick and a Ni bus bar are deposited to provide the top contact to the tandem cell.

The cell area and contacts are defined by a photolithography-etching procedure where the excess CdS and ITO are removed by a

concentrated HCl etch, the Ni bus bars are etched with 20% HNO_3, and the CdTe is etched with a 5% solution of Br-methanol. (All solutions are at room temperature.) This procedure yields 12 tandem cells each 3x3 mm^2 on a 2.5x2.5 cm^2 substrate. The cell has three terminals so the individual and tandem characteristics (J-V, spectral response, etc.) can be measured.

RESULTS

The J-V characteristics of the highest efficiency CdS/CdTe-CdS/$CuInSe_2$ tandem cell made to date are shown in Figure 2. Because of the three terminal construction, it is possible to simultaneously display the J-V characteristics of the individual devices as well. The basic device parameters are given in Table 5. The open circuit voltage of the tandem device is over 1 volt and the efficiency is over 3%. The low fill factor in the CdS/CdTe device and the tandem device is caused by the non-ohmic contact between the CdTe the Cu and ITO interconnect. This non-ohmic behavior can be seen in the J-V characteristics of Figure 2.

The collection efficiencies of the individual devices versus wavelength for the tandem structure, both with and without AM1 light bias, are shown in Figures 3 and 4. The change in collection efficiency of the CdS/CdTe device with the change in light bias is again primarily due to the contact problem at the CdTe cell interconnect layers. The lack of response in the CdS/$CuInSe_2$ device at wavelengths shorter than the CdTe bandgap is indicative of a well defined pinhole free tandem structure.

SUMMARY

The $CuInSe_2$/CdS-CdTe/CdS device demonstrates that a two cell multi-bandgap tandem structure can be made from single junction polycrystalline thin-film solar cells. The cell structure and production process must result in a transparent ohmic interconnect between the two cells and the process for making the second device must not adversely affect the initial cell. Within these restrictions it should be possible to build thin-film polycrystalline tandem devices with a substantially higher efficiency than their single junction counterparts.

ACKNOWLEDGEMENTS

The skilled technical contributions of E.Ashmead, S.Buchanan, C.Field, J.Hall, P.Lasswell, H.Wardell and J.Wheeler are gratefully acknowledged. The development of the $CuInSe_2$ process was greatly aided by R.B.Hall. The work was supported by DOE-SERI under subcontract #XL-3-03065-01.

REFERENCES

1. R. Taylor, "Materials and New Processing Technologies for Photovoltaics," ed. J. Dismukes et al., 161st Meeting of Electrochemical Society, Vol.82-8, 59 (1982).

2. A. Devos, J. Phys. D., Appl. Phys., 13, 839 (1980).

3. J. C. C. Fan, B-Y. Tsaur and B. J. Palm, Proceedings of the 16th IEEE Photovoltaic Specialists Conference, 1982 (New York: IEEE), p. 692.

4. S. M. Bedair, J. A. Hutchby, J. Chiang, M. Simons, and J. R. Hauser, Proceedings of the 15th IEEE Photovoltaic Specialists Conference, 1981 (New York: IEEE), p. 21.

5. G. Nakamura, K. Sato, H. Kondo, Y. Yukimoto, K. Shiruhata, Proceedings of the 4th E.C. Photovoltaic Solar Energy Conference, 1982 (Dordrecht-D. Reidel Publishing Co.), p. 616.

6. R. W. Birkmire, L. C. DiNetta, J. D. Meakin and J. E. Phillips, "$CuInSe_2$/CdS-CdTe/CdS Polycrystalline Tandem Solar Cells," to be published in the Proceedings of the 17th IEEE Photovoltaic Specialists Conference, (1984).

7. W. H. Bloss, J. Kimmerle, F. Pfisterer and W. H. Schock, "Thin-Film Tandem Solar Cells Based on II-VI Compounds," to be published in the Proceedings of the 17th IEEE Photovoltaic Specialists Conference, (1984).

8. J. C. C. Fan and B. J. Palm, Solar Cells, 12, 401 (1984).

9. R. A. Mickelsen and W. S. Chen, Proceedings of the 16th IEEE Photovoltaic Specialists Conference, 1982 (New York: IEEE), p. 781.

10. Y. Tyan and E. A. Perez-Albuerne, Proceedings of the 16th IEEE Photovoltaic Specialists Conference, 1982 (New York: IEEE), p. 794.

11. R. J. Matson, K. A. Emery and R. E. Bird, Solar Cells, 11, 105, 1984.

12. D. Bonnet and H. Rabenhorst, Proceedings of the 9th IEEE Photovoltaic Specialists Conference, 1972 (New York: IEEE), p. 129.

13. R. A. Mickelsen and W. S. Chen, Proceedings of the 15th IEEE Photovoltaic Specialists Conference, 1981 (New York: IEEE), p. 800.

TABLE 1

Optimum Efficiency for Multigap Cells
Under Unconcentrated Sunlight

n	Eff_{max} (%)	Eg_1 (eV)	Eg_2 (eV)	Eg_3 (eV)	Eg_4 (eV)
1	30	1.3	-	-	-
2	42	1.9	1.0	-	-
3	49	2.3	1.4	0.8	-
4	53	2.6	1.8	1.2	0.8
∞	68				

After Ref. 2

TABLE 2

Optimum Efficiency for Multigap Cells
Under Maximum Sunlight Concentration of 45,900:1

n	Eff_{max} (%)	Eg_1 (eV)	Eg_2 (eV)	Eg_3 (eV)	Eg_4 (eV)
1	40	1.1	-	-	-
2	55	1.7	0.8	-	-
3	63	2.1	1.2	0.6	-
4	68	2.5	1.6	1.0	0.5
∞	86				

After Ref. 2

TABLE 3

Practical Efficiency Limits For
CdS Based Thin-Film Devices

Device	V_{oc} (V)	J_{sc} @100mW/cm^2 (mA/cm^2)	FF (%)	Eff (%)
$CdS/CuInSe_2$	0.42	38	65	10
CdS/CdTe	0.86	18	80	12
$CdS/CdTe-CdS/CuInSe_2$	1.3	18	75	17

TABLE 4

Practical Efficiency Limits For
(CdZn)S Based Thin-Film Devices

Device x ~ 0.3	V_{oc} (V)	J_{sc} @100mW/cm^2 (mA/cm^2)	FF (%)	Eff (%)
$Cd_{1-x}Zn_xS/CuInSe_2$	0.62	40	65	16
$Cd_{1-x}Zn_xS/CdTe$	1.0	20	80	16
$(CdZn)S/CdTe-(CdZn)S/CuInSe_2$	1.6	18	75	21

TABLE 5

I-V Results of Tandem and Individual
Solar Cells After a 200°C,
7 Hour Air Heat Treatment

	V_{oc} (V)	J_{sc}* (mA/cm^2)	FF (%)	η (%)
T0008.4	1.020	6.5	40	3.0
40173.21T	0.683	8.3	30	1.9
31333.33T	0.336	6.1	46	1.1

* ELH solar simulator at 87.5 mW/cm^2

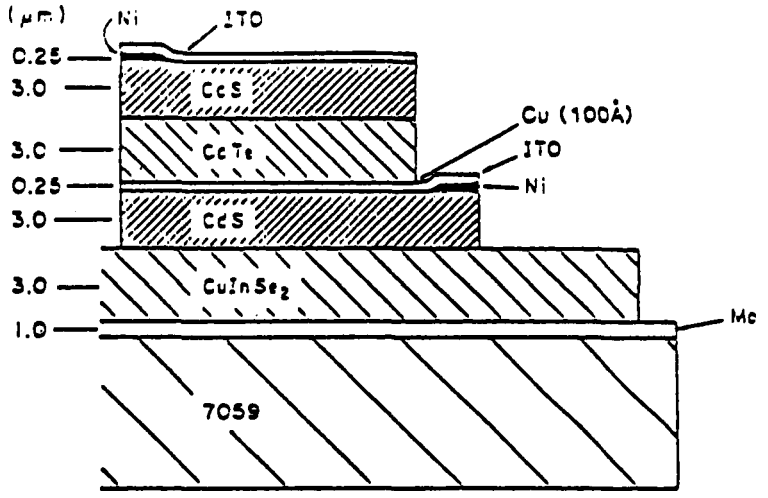

Figure 1. Cross-section of CdS/CdTe-CdS/$CuInSe_2$ polycrystalline cell.

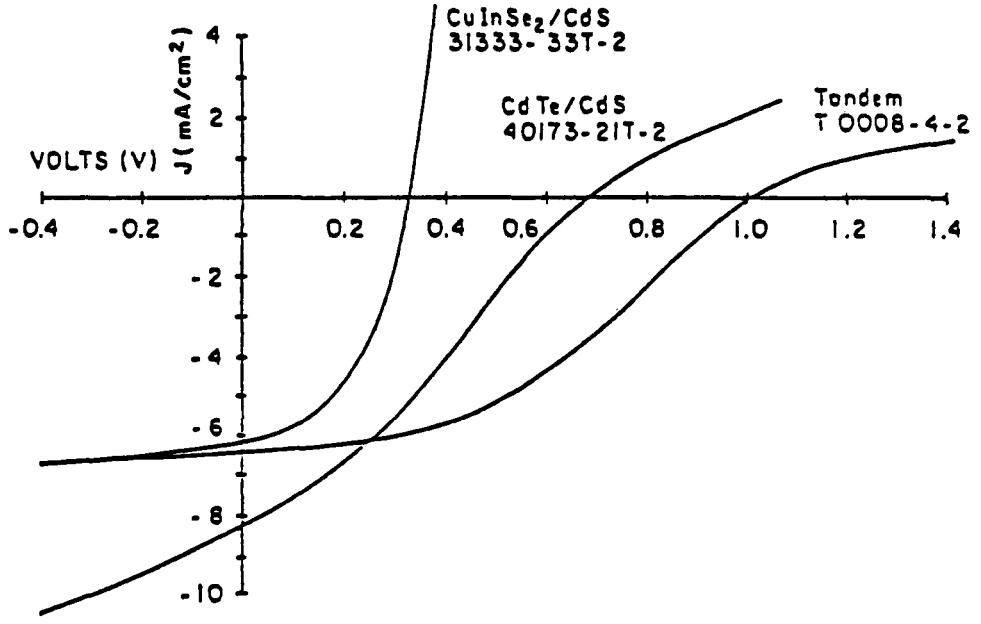

Figure 2. J-V characteristics of tandem on individual cells.